

The mitochondrial genome of the red icefish
 (*Channichthys rugosus*) casts doubt on its
 species status

Moritz Muschick^{1,2*}, Ekaterina Nikolaeva³, Lukas Rüber^{1,4}
 and Michael Matschiner^{5*}

^{1*}Aquatic Ecology & Evolution, Institute of Ecology and
 Evolution, University of Bern, Bern, 3012, Switzerland.

²Department of Fish Ecology & Evolution, EAWAG, Swiss
 Federal Institute for Aquatic Science and Technology,
 Kastanienbaum, 6047, Switzerland.

³Ichthyology Laboratory, Zoological Institute of the Russian
 Academy of Sciences, St. Petersburg, 199034, Russia.

⁴Naturhistorisches Museum Bern, Bern, 3005, Switzerland.

⁵Natural History Museum, University of Oslo, Oslo, 0562, Norway.

*Corresponding author(s). E-mail(s): Moritz.Muschick@eawag.ch;
michael.matschiner@nhm.uio.no;

Contributing authors: ekaterina.nikolaeva@zin.ru;
lukas.ruber@nmbe.ch;

Abstract

Antarctic notothenioid fishes are recognized as one of the rare examples
 of adaptive radiation in the marine system. Withstanding the freezing
 temperatures of Antarctic waters, these fishes have diversified into over
 100 species within no more than 10-20 million years. However, the ex-
 act species richness of the radiation remains contested. In the genus
Channichthys, between one and nine species are recognized by different
 authors. To resolve the number of *Channichthys* species, genetic infor-
 mation would be highly valuable; however, so far, only sequences of a
 single species, *C. rhinoceratus*, are available. Here, we present the nearly
 complete sequence of the mitochondrial genome of *C. rugosus*, obtained
 from a formalin-fixed museum specimen sampled in 1974. This sequence

2 *Mitochondrial genome of the red icefish*

047 differs from the mitochondrial genome of *C. rhinoceratus* in no more
 048 than 27 positions, suggesting that the two species may be synonymous.

049 **Keywords:** icefish, Antarctica, species richness, taxonomy, museomics,
 050 mitochondrial genome

051
 052
 053
 054

1 Introduction

056 The diversification of fishes of the perciform suborder Notothenioidei in
 057 Antarctic waters is a rare example of adaptive radiation in the marine envi-
 058 ronment (Clarke & Johnston, 1996; Eastman, 2005; Matschiner et al., 2015;
 059 Near et al., 2012; Rüber & Zardoya, 2005). The radiating group of noto-
 060 thenioid fishes is composed of five families (Nototheniidae, Harpagiferidae,
 061 Artedidraconidae, Bathydraconidae, and Channichthyidae; jointly called "Cry-
 062 onotothenioidea" (Near et al., 2015)) that together include over 100 species,
 063 distributed primarily on the shelf areas surrounding Antarctica and sub-
 064 Antarctic islands (Eastman & Eakin, 2021; Gon & Heemstra, 1990). The
 065 validity of most species within this radiation is well established and in many
 066 cases corroborated by genetic data. However, in other cases, species are known
 067 only from few specimens and distinguished from congeners based on minute
 068 morphological differences alone. One such example is the genus *Pogonophryne*
 069 (Artedidraconidae), for which close to twenty species have been described
 070 within the last four decades (Eastman & Eakin, 2021), primarily on the basis of
 071 variation in the morphology of the mental barbel (*e.g.* Spodareva & Balushkin,
 072 2014). This species richness within *Pogonophryne* could not be confirmed in a
 073 recent genetic analysis, which instead led to the synonymization of 24 out of
 074 29 valid species (Parker, Dornburg, Struthers, Jones, & Near, 2022).

075 Outside *Pogonophryne*, the validity of species described in the genus *Chan-*
 076 *nichthys* (Channichthyidae) remains particularly questionable. As many as
 077 nine species have been recognized, including the unicorn icefish (*C. rhinocera-*
 078 *tus* Richardson, 1844), the red icefish (*C. rugosus* Regan, 1913), the sailfin pike
 079 (*C. velifer* Meisner, 1974), and six species described by Shandikov between
 080 1995 and 2011 (Aelita icefish, *C. aelitae*; big-eyed icefish, *C. bospori*; pygmy
 081 icefish, *C. irinae*; charcoal icefish, *C. panticapaei*; green icefish, *C. mithridatis*;
 082 and robust icefish, *C. richardsoni*) (Shandikov, 1995a, 1995b, 2008, 2011)
 083 (Table 1). All species of the genus are endemic to the Kerguelen-Heard plateau
 084 and appear to share largely overlapping distributions (Shandikov, 2011), im-
 085 plying that they either represent a small radiation on their own, or that at
 086 least some of the described taxa are *de facto* morphs of one and the same
 087 species. The members of the genus are morphologically similar, with total
 088 lengths around 30–50 cm, a wide and spatulated snout, a tall first dorsal fin,
 089 and the rostral spine that gave its name to the the first described species, *C.*
 090 *rhinoceratus* (Richardson, 1844).

091
 092

The second-oldest species, *C. rugosus*, was described on the basis of two specimens that were found to differ from the known *C. rhinocerus* specimens in eye diameter, roughness of the head, the position of supraorbital edges, and the length of the maxillary (Regan, 1913). As additional specimens became available, the diagnosis of the two species became refined (Norman, 1937), but the lack of clearly species-defining traits led some authors to question their separation even before further members of the genus were described (Hureau, 1964). The third species to be described was *C. velifer* (Meisner, 1974), which was claimed to differ from *C. rhinocerus* in the number of spines of the first dorsal fin and the presence of a single median series of bony plates on the posterior part of the body (Meisner, 1974). However, most of the specimens assigned to this new taxon were females, suggesting that sexual dimorphism could have explained the observed differences (Gon & Heemstra, 1990). The six remaining described species were added to the list to accommodate previously unseen combinations of ray numbers, interorbital width, fin membrane height, and a duplicated row of gill rakers, among others (Shandikov, 1995a, 1995b, 2008, 2011). In most cases, these species were described on the basis of few specimens only.

Table 1 Species described in genus *Channichthys*

Name	Authority	Year	# specimens
<i>C. rhinocerus</i>	Richardson	1844	1,093
<i>C. rugosus</i>	Regan	1913	26
<i>C. velifer</i>	Meisner	1974	83
<i>C. panticapaei</i>	Shandikov	1995	72
<i>C. aelitae</i>	Shandikov	1995	3
<i>C. bospori</i>	Shandikov	1995	5
<i>C. irinae</i>	Shandikov	1995	23
<i>C. mithridatis</i>	Shandikov	2008	29
<i>C. richardsoni</i>	Shandikov	2011	18

Species considered valid by Nikolaeva (2021) are marked in bold. The last column specifies the minimum number of specimens present in museum collections, based on the GBIF database (<https://www.gbif.org>) and a literature review.

To address a felt demand for a “complete overhaul” (Duhamel, Gasco, & Davaine, 2005; Eastman & Eakin, 2021) of the systematics of the genus *Channichthys*, Nikolaeva and Balushkin began a series of investigations based on comprehensive comparisons of specimens in the collections of the Zoological Institute of the Russian Academy of Sciences in Saint Petersburg, the Ukrainian National Museum of Natural History in Kyiv, and the British Natural History Museum in London. Their analyses indicated that the duplicate gill rakers observed in *C. rhinocerus*, *C. panticapaei*, *C. bospori*, and *C. irinae*, but also in more distantly related icefishes, are a rather labile character (Balushkin & Nikolaeva, 2015), leading them to suggest the synonymization

of the latter three *Channichthys* species (Nikolaeva, 2019). Their work further resulted in redescrptions of *C. velifer* (Nikolaeva & Balushkin, 2019), *C. rhinocerotus* (Nikolaeva, 2020), and *C. rugosus* (Nikolaeva, 2021), as well as the suggested synonymization of *C. aelitae*, *C. mithridatis*, and *C. richardsoni* with *C. rhinocerotus* (Nikolaeva, 2020).

Thus, according to Nikolaeva and Balushkin, the following four species are currently recognized in the genus *Channichthys*: *C. rhinocerotus*, *C. rugosus*, *C. velifer*, and *C. panticapaei*. The redescrbed *C. rugosus* differs from *C. rhinocerotus* in four characters: greater height of the anterior dorsal fin, a fin membrane extending to the apexes of the longest rays, a narrower and concave interorbital space, and a more uniformly reddish body color (Nikolaeva, 2021). *Channichthys rugosus* can be further distinguished from *C. velifer* by numbers of fin rays in the first dorsal and the pectoral fin, bone plaques on the lateral line, and its coloration. Additionally, *C. panticapaei* was said to differ from *C. rugosus* in having a duplicated row of gill rakers and a more brownish-black coloration (Nikolaeva, 2021).

To complement the morphological analyses of *Channichthys* species and further test their validity, genetic data would be essential. Unfortunately, however, molecular information is so far only available for a single species, *C. rhinocerotus*. The genetic data available for this species include a set of ten nuclear markers commonly used in phylogenetic studies, cytochrome c oxidase I (*CO1*) barcodes (Smith et al., 2012), and the recently published complete sequence of a mitochondrial genome with a length of 17,408 bp (Andriyono et al., 2019), as well as restriction-site associated DNA (RAD) markers (Near et al., 2018). These sequences are available from the National Center for Biotechnology Information (NCBI). For the other three potentially valid species of the genus, the unavailability of sequence information is at least in part due to the rarity of suitable tissue samples. To the best of our knowledge no more than 3–72 specimens are present for these species in museum collections (Table 1). Moreover, most specimens of these species were caught decades ago and fixed in formalin, which leads to degradation and chemical modification of DNA, making the recovery of genetic information challenging. To overcome this limitation, protocols for DNA extraction and sequencing library preparation tailored for formalin-fixed specimens have recently become available and proved to be remarkably successful (Gansauge, Aximu-Petri, Nagel, & Meyer, 2020; Gansauge et al., 2017; Gould, Fritts-Penniman, & Gaisner, 2021).

Here, we apply recently developed methods to retrieve DNA sequences from a specimen of *C. rugosus* that was collected and formalin-fixed in 1974, and stored in 70 percent ethanol since. Modifications to a standard DNA extraction protocol from animal tissue maximise the yield of short DNA fragments, while application of a single-stranded DNA library preparation method (Gansauge et al., 2020, 2017) allows to convert even minute amounts of degraded DNA into sequencing libraries. We reconstruct the complete sequence of the specimen's mitochondrial genome based on Illumina read data, and compare this sequence to the mitochondrial genome of *C. rhinocerotus* to assess the genetic divergence

between these two species. We find that the two mitochondrial genomes are nearly identical, with only 27 nucleotide differences between them. Such close similarity lends support to the synonymy of the two species *C. rugosus* and suggests that, like *Pogonophryne*, *Channichthys* comprises fewer differentiated species than previously thought.

2 Materials and methods

2.1 Sampling

The *C. rugosus* specimen used for sequencing was collected on 28.06.1974 during voyage 7 of the Soviet scientific trawler ‘Skif’ (‘Скиф’). It was obtained by bottom-trawling (trawl 188) on the Kerguelen shelf, at a depth of 115–120 m to the North-East of the Kerguelen Islands (48°34’1 S, 70°37’1 E). The specimen (ZIN 56294) has a standard length of 252 mm and is located in the collection of the Zoological Institute of the Russian Academy of Sciences in Saint Petersburg, Russia. It was formalin-fixed upon arrival in Saint Petersburg and remained in 40% formalin for several years before being transferred to 70% ethanol. The specimen had been identified as *C. rugosus* based on the height of its first dorsal fin, the shape of its interorbital space, its body coloration, numbers of fin rays, and the absence of a second row of gill rakers on the first gill arch (Nikolaeva, 2021).



Figure 1 *Channichthys rugosus* specimen ZIN 56294. Photograph (a) and x-ray image (b) of the *C. rugosus* specimen used for DNA extraction. The specimen has a standard length of 252 mm.

231 **2.2 DNA extraction and sequencing**

232 A small piece of muscle tissue (5.8 mg dry weight) was dried in a vacuum cen-
233 trifuge and immersed in lysis buffer (260 μ L ATL buffer (Qiagen) and 40 μ L
234 Proteinase K [20 mg/mL]). Two extraction negative control reactions received
235 the same lysis buffer, but did not contain sample. After 24 h incubation at 56
236 $^{\circ}$ C, the lysates were centrifuged at 17,000 \times g for 5 minutes and 300 μ L su-
237 pernatant mixed with 3000 μ L Buffer PB (Qiagen). The mixtures were loaded
238 onto Minelute silica columns (Qiagen) in steps of 600 μ L, then washed twice
239 with 600 μ L Buffer PE (Qiagen). Centrifugation was carried out for 1 minute
240 each at 8,000 \times g, which is lower than recommended by the manufacturer, in
241 order to increase the retention of short DNA fragments. The columns were dry
242 spun 1 minute at 16'000 \times g to remove residual wash buffer. To elute the DNA,
243 50 μ L Buffer AE (Qiagen) were placed directly onto the silica membrane, in-
244 cubated for 10 minutes and centrifuged at 16,000 \times g for 2 minutes. DNA
245 concentration was determined using 5 μ L of the extract in a Qubit dsDNA
246 High Sensitivity assay. The sample yielded 6.6 ng/ μ L, while the extraction
247 negatives contained 0.0244 ng/ μ L or were below the detection threshold of
248 0.02 ng/ μ L, respectively. Eight μ L of the extract (=52.8 ng DNA) and 30 μ L
249 each of the negative controls were then used to build Illumina sequencing li-
250 braries by single-stranded DNA library preparation as described by [Gansauge](#)
251 [et al. \(2020, 2017\)](#), using the same reagents as listed in [Gansauge et al. \(2020\)](#).
252 Briefly, the DNA extract and two extraction negative controls, along with
253 one library negative control (water) and one library positive control (0.1 pmol
254 of oligonucleotide CL104) were used for five separate library build reactions.
255 Furthermore, all reactions received 10 amol CL104 as internal control. Sam-
256 ples were dephosphorylated and the 3'-adapter (TL181/TL110) attached by
257 splinted ligation. Adapter molecules were bound to streptavidin-coated mag-
258 netic beads which were carried through the reactions and washed after each
259 enzymatic reaction. An adapter-complementary primer (CL128) was used to
260 prime the fill-in reaction, creating 5'-blunt-ended double stranded molecules.
261 Another ligation attached the second adapter (CL53/TL178). Libraries were
262 eluted into 50 μ L Tween-20 supplemented Tris-EDTA buffer (i.e. TET buffer)
263 by heat denaturation. 1 μ L each of a 1:50 dilution of libraries was used in two
264 qPCR assays to determine control molecule numbers and required PCR-cycle
265 numbers for amplification. The remaining 49 μ L of libraries, with the exception
266 of the positive library control, were then uniquely dual indexed (7 bp index
267 length) ([Kircher, Sawyer, & Meyer, 2012](#)) and amplified until the end of the
268 exponential phase, then purified using the Minelute PCR purification kit (Qi-
269 agen). Libraries were pooled and size-selected to 160–250 bp on a Blue Pippin
270 instrument using a 3% cassette with internal markers. The selected size frac-
271 tion was measured with both, the Qubit dsDNA High Sensitivity assay and
272 the TapeStation HS1000 assay to adjust the input molarity for the sequenc-
273 ing run. The pool was then sequenced on an Illumina NextSeq500 instrument
274 using a high-output single-end 75 bp read length kit with custom primers for
275 read 1 (CL72) and index 2 (Gesaffelstein) ([Paijmans et al., 2017](#)).
276

Raw read files were demultiplexed using bcl2fastq v.2.19.1 (<https://support.illumina.com/sequencing/sequencing-software/bcl2fastq-conversion-software.html>), allowing for a maximum combined distance of 1 between barcodes, and saved to fastq format. In the same step, prevalent adapter sequences were trimmed from the ends of reads, and reads under 20 bp of length were omitted.

To ensure the presence of endogenous reads, we matched each read to the NCBI non-redundant (NR) sequence database (downloaded on 12 February 2022) with the BLASTX algorithm as implemented in Diamond v.2.0.4 (Altschul, Gish, Miller, Myers, & Lipman, 1990; Buchfink, Xie, & Huson, 2015). The resulting taxon assignments were plotted with MEGAN v.6.21.4 (Huson et al., 2016).

2.3 Reference-based sequence analysis

We mapped reads to the *C. rhinocerotus* mitochondrial genome (Genbank accession number NC.057120) using BWA v.0.7.17 (Li & Durbin, 2010), with its “aln” algorithm and the maximum fraction of missing alignments set to 0.05. The *C. rhinocerotus* mitochondrial genome was obtained from an individual that was collected in 2018 from Antarctic Subarea 58.5.2 (Heard Island and McDonald Island; Sapto Andriyono and Hyun-Woo Kim, priv. comm.). Resulting alignments were filtered to a Phred-scaled mapping quality of 25 or higher with Samtools v.1.9 (Li et al., 2009). Duplicated reads, e.g. from PCR duplicates, were flagged with Picard’s v.2.21.3 (<http://broadinstitute.github.io/picard/>) MarkDuplicate function and filtered with Samtools. Sites with a minimum read depth of 3 were consensus called using ANGSD v.0.933 (Korneliussen, Albrechtsen, & Nielsen, 2014). To recover the terminal positions of the sequence, the first 200 bp of the reference were cut and appended, and the mapping repeated. Regions of low-complexity and larger repeats exceeding the read length were edited manually or replaced with “N” for the length of the reference, as described in the Results section. The degradation state of DNA was assessed by inspection of the distribution of read lengths and analysis of substitution frequencies per base position within reads, using mapDamage v.2.0.8 (Jónsson, Ginolhac, Schubert, Johnson, & Orlando, 2013).

2.4 Reference-independent sequence analysis

To exclude potential reference bias, we also performed analyses of the mitochondrial genome of *C. rugosus* based on *de novo* assembly. We performed local assembly of individual mitochondrial markers with aTRAM v.2.0 (Allen, LaFrance, Folk, Johnson, & Guralnick, 2018). As queries, we used nucleotide and protein sequences from all mitochondrial genomes available on NCBI. To identify these notothenioid mitochondrial genomes on NCBI, we used the search string ““Notothenioidi”[Organism] AND (“mitochondrial”[Title] OR “mitochondrion”[Title]) AND “complete genome”[Title]” on 4 December 2021. This set of mitochondrial genomes included the one for *Channichthys*

323 *rhinoceratus* and 40 other unique mitochondrial genomes. From each of these
324 41 mitochondrial genomes, we extracted each gene (rRNA, tRNA, or protein-
325 coding) in nucleotide format, and protein-coding features in amino-acid format,
326 and used all of these in aTRAM analyses. All aTRAM analyses were performed
327 separately with seven different e-value thresholds (1e-2, 1e-3, 1e-4, 1e-5, 1e-6,
328 1e-8, 1e-10) for the BLASTN and TBLASTN v.2.10.1 (Altschul et al., 1990)
329 searches that aTRAM runs internally. As the assembler tool internally em-
330 ployed by aTRAM, we selected Trinity v.2.10.0 (Grabherr et al., 2011). Each
331 aTRAM analysis was continued for 20 iterations.

332 All contigs produced by aTRAM were jointly used as input for a sec-
333 ond assembler tool, MIRA v.4.9.6 (Chevreux, Wetter, & Suhai, 1999). We
334 set MIRA’s “nasty repeat ratio” to 25 (“-KS:nrr=25”), the “maximum
335 megahub ratio” to 40 (“-SK:mmhr=40”), specified the lack of quality in-
336 formation (“-AS:epoq=no”), and turned off the checks for average coverage
337 (“-NW:cac=no”) and maximum read name length (“-NW:cmrnl=warn”), ac-
338 cording to the format of the input data. The contigs produced by MIRA (or
339 their reverse complements) were then individually aligned to the mitochon-
340 drial genome for *C. rhinoceratus* with MAFFT v.7.470, using a gap opening
341 penalty of 2, a gap extension penalty of 1, and the program’s “6merpair” and
342 “addfragments” options.

343

344 2.5 Comparative analyses

345

346 The reference-based and reference-independent mitochondrial genome se-
347 quences for *C. rugosus* were compared visually using AliView v.1.2.6 (Larsson,
348 2014). Nucleotide sequences of the 13 protein-coding genes were extracted
349 from the mitochondrial genome of *C. rugosus* and all other notothe-
350 nioid mitochondrial genomes and aligned per gene with MAFFT. The 13
351 alignments were concatenated and a distance matrix was calculated from
352 the concatenated alignment with the Python script “convert.py” (avail-
353 able from GitHub: https://github.com/mmatschiner/supergenes/blob/main/gadidae_phylogenomics/src/convert.py), ignoring all sites with missing data.
354 The concatenated alignment was further used for maximum-likelihood phy-
355 logenetic inference with IQ-TREE v.2.1.2 (Minh et al., 2020), applying
356 the program’s automated substitution model selection and 1000 ultrafast
357 bootstrap (Minh, Nguyen, & von Haeseler, 2013) iterations.

359 To gain a more complete view of sequence variation in *Channichthys*, we
360 took advantage of the *CO1* barcode sequences available on NCBI (Smith et
361 al., 2012). We downloaded these sequences and aligned them together with
362 the homologous sequences extracted from the mitochondrial genomes of *C.*
363 *rhinoceratus* and *C. rugosus*, using MAFFT. To illustrate the *CO1* sequence
364 variation in *Channichthys*, we first applied maximum-likelihood phylogenetic
365 inference with IQ-TREE and then used the estimated phylogeny jointly with
366 the sequence alignment to draw a haplotype genealogy graph with the program
367 Fitchi v.1.1.4 (Matschiner, 2016).

368

3 Results

3.1 Sequencing

For the *C. rugosus* specimen, a total of 63,158,791 reads passed initial trimming and length filtering. For extraction negative controls 1 and 2 (exneg 1, exneg 2), and library negative control (libneg), the number of reads were 22,393,754, 21,343,774 and 3,080,057, respectively. Analysis with Diamond and MEGAN assigned a substantial proportion of the reads to Notothenioidei and confirmed that these were endogenous (Fig. 4).

3.2 Reference-based sequence analysis

Mapping to the *C. rhinoceratus* mitochondrial genome generated 48,313 hits, corresponding to 0.0765% of total reads. After filtering duplicates, 18,687 unique reads were used for further analysis. These reads had an average length of 32.98 bp, with only 0.1% of reads being 70 bp or longer. Figure 2 shows the distribution of read lengths of hits. Negative controls produced 5 (exneg 1), 5 (exneg 2), and 1 unique hit (libneg), which weren't analysed further. The resulting coverage had an average depth of 35.4 and extended over 98.1% of the reference. The alignment showed two apparent gaps in the D-loop and spurious alignments directly adjacent to them, therefore positions 15,192–15,294 and 16,856–17,262, respectively, were called as "N" for the length of the reference. A 14-mer C repeat at reference positions 15,986–15,999 was spanned by two reads only, both indicating an indel with one fewer repeat in *C. rugosus*, which was called manually. Mapped reads showed an elevated rate of C to T changes in both their 3'- and 5'-ends, a pattern of cytosine deamination that is typical for degraded DNA (Fig. 3).

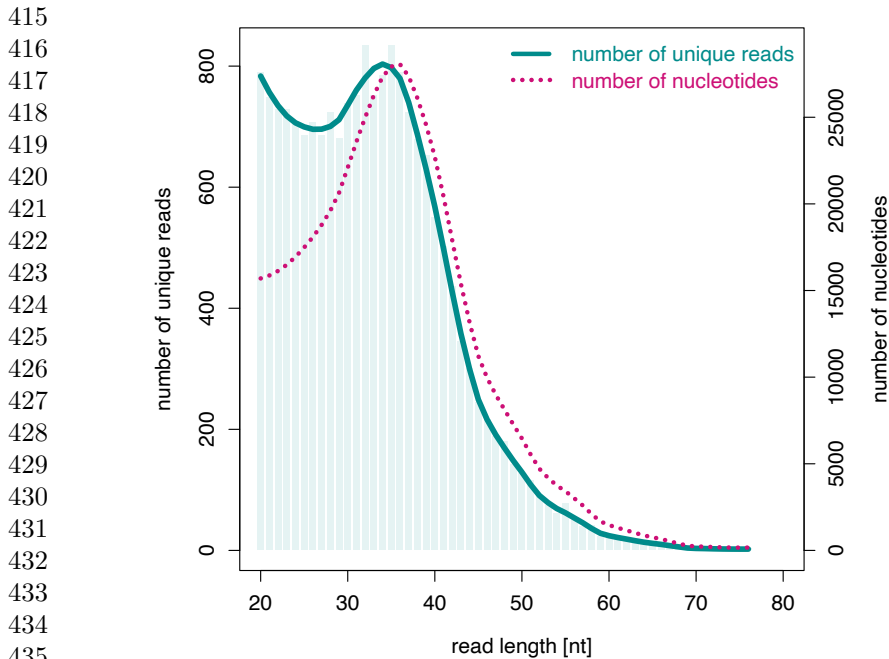
3.3 Reference-independent sequence analysis

Assembly with MIRA produced 14 contigs with lengths between 317 and 1471 basepairs (bp) (mean length: 677.4 bp). One of these contigs overlapped fully with another one, and two other contigs overlapped by 13 bp. The total length of the mitochondrial genome covered by these contigs was 9,849 bp. No nucleotide differences were observed between overlapping contigs.

3.4 Comparative analyses

Comparison of the reference-based and the reference-independent mitochondrial genome sequences showed that these were completely identical across the 9,849 bp covered by both. Compared to the mitochondrial genome of *C. rhinoceratus*, the reference-based sequence differed at 27 sites (Table 2). Seventeen of these nucleotide differences were within regions also covered by the reference-independent sequence for *C. rugosus*, and all of these were confirmed by that sequence. The differences between the *C. rhinoceratus* and *C. rugosus* mitochondrial genomes included five transitions (two A/C, one G/C, one

369
370
371
372
373
374
375
376
377
378
379
380
381
382
383
384
385
386
387
388
389
390
391
392
393
394
395
396
397
398
399
400
401
402
403
404
405
406
407
408
409
410
411
412
413
414



437 **Figure 2** Distribution of read lengths of hits to the *C. rhinoceratus* mitochondrial
438 genome. The solid line and bars indicate the number of hits for a given read length, the
439 dotted line indicates the amount of data in nucleotides gathered from reads of a given length.

440 G/T, and one T/G substitution) and 21 transversions (seven A/G, two C/T,
441 six G/A, and six T/C substitutions), as well as one C/- indel. The nucleotide
442 differences were distributed unevenly across the mitochondrial genome and
443 mostly found in the *ND6* gene and the D-loop region (Fig. 5). Compared to
444 the mitochondrial genome-wide background of 0.0011 substitutions per bp, the
445 *ND6*/D-loop region had an elevated divergence of 0.0065 substitutions per bp.
446

447 Phylogenetic inference with IQ-TREE based on protein-coding mitochondrial
448 sequences grouped the two *Channichthys* genomes with full bootstrap
449 support. The two taxa were separated only by very short branches that had
450 a combined length of 0.0012 substitutions per bp. The *Channichthys* mito-
451 chondrial genomes were most similar to those of *Chionobathyscus dewitti* and
452 *Cryodraco antarcticus*, with which they formed a clade that also received full
453 bootstrap support. This clade appeared as the sister group to a clade formed
454 by the mitochondrial genomes of *Chaenodraco wilsoni* and three members of
455 the genus *Chionodraco*, albeit with low bootstrap support of 70% (Fig. 6).

456 The haplotype genealogy graph for 14 available *Channichthys CO1* se-
457 quences showed that eleven of them shared the same haplotype. Three other
458 haplotypes differed by a single substitution from the majority haplotype and
459 were each represented by a single individual. One of these three private hap-
460 lotypes was found found in the published mitochondrial genome sequence for

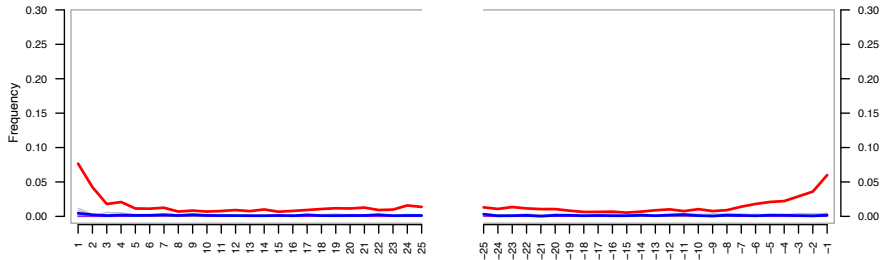


Figure 3 Frequency of post-mortem C to T changes by nucleotide position within reads. Deaminated cytosines are being read as thymine and are especially prevalent at molecule ends. Red line: relative frequency of T by position in read from 5'-end (left) and 3'-end (right), blue line: relative frequency of A. Here, the deamination signal manifests only as C to T, and not G to A, because single-stranded, rather than double-stranded DNA library preparation was used.

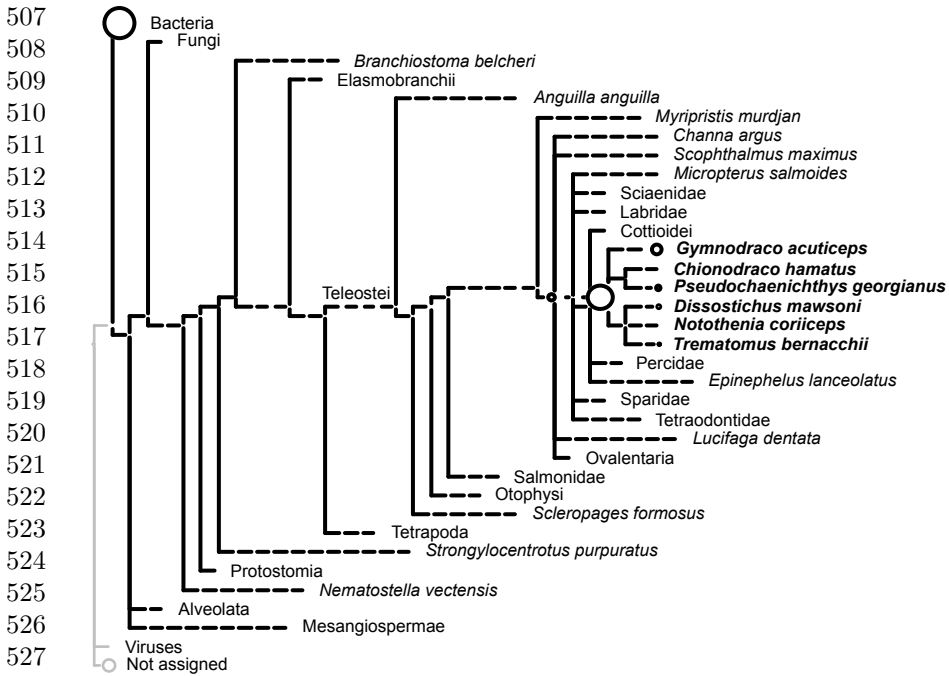
C. rhinocerotus, while the *C. rugosus* mitochondrial genome had the majority haplotype (Fig. 7).

4 Discussion

Our comparison of the mitochondrial genomes of *C. rhinocerotus* and *C. rugosus* showed that these two mitochondrial genomes are highly similar, with only one indel, 26 nucleotide substitutions and six amino-acid substitutions between them. The sequence divergence is 0.16%, and most of this divergence is concentrated in the *ND6*/D-loop region where the divergence reaches 0.65%. Despite very short read lengths, reconstruction of *C. rugosus*' mitochondrial genome was possible, except for two loci in the *ND6*/D-loop region. Those are most likely repeats that were too large to be spanned by single reads and could not be mapped correctly. While larger rearrangements of nothotenioid mitochondrial genomes have been reported by Papetti et al. (2021), gene order was shown to be identical for eight of the species in figure 6 (all except *Chionobathyscus dewitti*, *Cryodraco antarcticus*, and *Channichthys* sp.). Hence, while possible, the gaps in the alignments are unlikely to be caused by rearrangements or larger indels, and are probably artifacts due to short read length. This highlights a shortcoming of the use of degraded DNA, where read lengths are usually limited by DNA molecule lengths rather than by sequencing technology, making the detection of structural variants challenging.

Analysis of post-mortem damage shows a robust pattern of cytosine deamination in single-stranded overhangs at molecule ends, manifesting as C to T changes in the sequencing data. Given the appreciable depth of coverage, however, we consider it very unlikely that any position was called erroneously due to this damage. Here, only C to T changes are seen as we used single-stranded DNA library preparation. In double-stranded DNA library preparation, deaminated cytosines would also be apparent as G to A changes in the sequencing data. The presence of this deamination signal can be interpreted as evidence for the authenticity of the sequences, as modern contamination would not show

461
462
463
464
465
466
467
468
469
470
471
472
473
474
475
476
477
478
479
480
481
482
483
484
485
486
487
488
489
490
491
492
493
494
495
496
497
498
499
500
501
502
503
504
505
506



529 **Figure 4 Taxonomic assignment of individual reads.** Reads were mapped to the
530 NCBI non-redundant (NR) database. The sizes of circles on internal and terminal nodes
531 are proportional to the numbers of reads mapping to the corresponding taxon; a single read
532 mapped to taxa without visible circles.

533 it. However, this is more relevant for ancient samples, for which the age of
534 endogenous DNA and *ex situ* contamination would be very different, and for
535 cases where contamination is more likely to be confused with endogenous se-
536 quences, such as ancient human samples. Here, contamination is unlikely to
537 affect our results, as negative controls didn't produce concerning numbers of
538 reads mapping to the reference, and no other samples or DNA were handled in
539 the laboratory environment which couldn't be readily distinguished from our
540 sample.

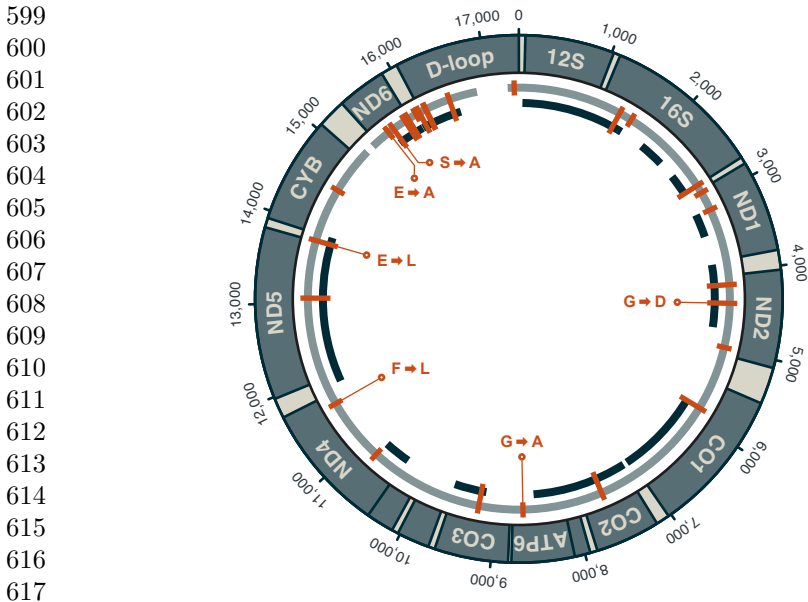
541 The available molecular data for the genus *Channichthys* does not allow
542 us to perform a formal genetic species delimitation analysis as was recently
543 done for *Pogonophryne* (Parker et al., 2022). Nevertheless, a comparison of
544 the divergence between the two *Channichthys* mitochondrial genomes with the
545 levels of between- and within-species sequence divergence in other notothenioid
546 fishes can inform about the existence of one or several species within the genus.
547 As shown in Fig. 6, the divergence within *Channichthys* is far smaller than
548 that between any other pairs of *Channichthyidae* species. Besides *Channichthys*
549 *rhinoceratus* and *C. rugosus*, the most closely-related species (judged on the
550 basis of their mitochondrial genomes) appear to be *Chionodraco hamatus* and
551 *Chionodraco rastrispinosus*. However, despite their recent divergence around
552

Table 2 Nucleotide substitutions and indel between *Channichthys* mitochondrial genomes

Site	Nucleotide substitution	Codon position	Codon substitution	Amino-acid substitution
1379	a/g			
1552	c/t			
2784	a/g			
2893	a/g	3	cta/ctg	
3145	g/c	3	ctg/ctc	
4165	t/c	3	att/atc	
4410	g/a	2	ggc/gac	G/D
4994	a/g	1	acc/gcc	T/A
5857	g/a	3	tgg/tga	
7586	a/g	3	gaa/gag	
8650	g/a	2	ggc/gac	G/A
9234	t/c	3	ctt/ctc	
10761	g/a	3	acg/aca	
11617	t/c	1	ttt/ctt	F/L
13006	t/c	3	gct/gcc	
13832	g/a	1	gag/aag	E/L
14550	a/c	3	gga/ggc	
15568	t/g	2	gag/gcg	E/A
15647	a/c	1	tca/gca	S/A
15831	a/g	3	gct/gcc	
15882	a/g	3	tgt/tgc	
15999	c/-			
16049	c/t			
16138	g/t			
16147	g/a			
16477	t/c			
17347	t/c			

a million years ago (Colombo, Damerau, Hanel, Salzburger, & Matschiner, 2015), the mitochondrial genomes of these two species are connected by a total branch length of 0.019 substitutions per bp, around 16 times as long as the branches connecting the two *Channichthys* mitochondrial genomes. Of note, the two *Chionodraco* species appear not to be fully separated, given that hybrids and signals of introgression have been observed (Schiavon et al., 2021).

On the other hand, the divergence between the two *Channichthys* mitochondrial genomes is comparable to the within-species divergence in other notothenioid species. Mitochondrial genomes of two individuals are available for five notothenioid species: *Trematomus borchgrevinkii*, *Notothenia coriiceps*, *Notothenia rossi*, *Chaenodraco wilsoni*, and *Chionodraco hamatus*. These two genomes per species differ by 16–92 substitutions and 3–22 indels across the mitochondrial genome, or by 11–69 substitutions and 2–10 indels when the *ND6* / D-loop region is excluded (Table 3). The divergence of the two *Channichthys* mitochondrial genomes is close to or below the lower ends of these ranges, considering that we found these two genomes to differ in 26 nucleotide substitutions (17 outside the *ND6* / D-loop region) and no indels



618 **Figure 5 Mitochondrial genome of *C. rugosus*.** Coordinates on the outside of the
619 circle are given in units of basepairs. The gray inner circle indicates the nearly full coverage
620 achieved in the reference-based analysis. Two gaps with a total length of 510 bp remain
621 in this sequence between positions 15,192 and 15,294, and between positions 16,856 and
622 17,262. The black fragments inside the gray circle show the positions of contigs from the
623 reference-independent approach. Substitutions compared to the mitochondrial genome of
624 *C. rhinoceratus* (NCBI accession NC_057120) are marked in orange, and non-synonymous
625 substitutions are labelled with the resulting amino-acid change.

625
626 were observed. In contrast, the two most-closely related pairs of sister species
627 within Channichthyidae (*Chionodraco hamatus*, *Chionodraco rastrospinosus*,
628 and *Chionobathyscus dewitti*, *Cryodraco antarcticus*; Fig. 2) differ by 421–540
629 substitutions and 25–34 indels (253–272 substitutions and 6–11 indels when the
630 *ND6* / D-loop region is excluded; Table 3). Thus, the divergence of the mito-
631 chondrial genomes of *Channichthys rhinoceratus* and *C. rugosus* is consistent
632 with the existence of a single species within the genus *Channichthys* (Eastman
633 & Eakin, 2021). If this result should be confirmed by further molecular data,
634 *Channichthys rugosus* may need to be synonymized with *C. rhinoceratus*.

635 Low divergence in mitochondrial genome sequence can be indicative of
636 a close – e.g. intraspecific – phylogenetic relationship, but could also be
637 due to alternative scenarios. Mitochondrial capture, where one lineage fixes
638 the mitochondrial genome received from another by introgression, can result
639 in two valid, reproductively largely isolated species with appreciable
640 nuclear genome divergence having no or little mitochondrial genome diver-
641 gence. This phenomenon can also apply to large, rapidly diversifying clades
642 where many species have arisen from nuclear genomic diversity created through
643 hybridisation of divergent ancestral lineages, for example in Lake Victoria’s
644

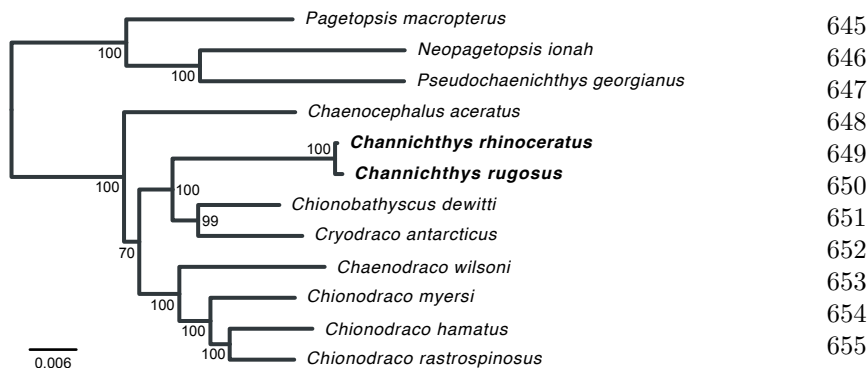


Figure 6 Mitochondrial phylogeny of Channichthyidae. Maximum-likelihood phylogeny of all available mitochondrial genomes for Channichthyidae. Short branches connect *Channichthys rhinoceras* and *C. rugosus*.

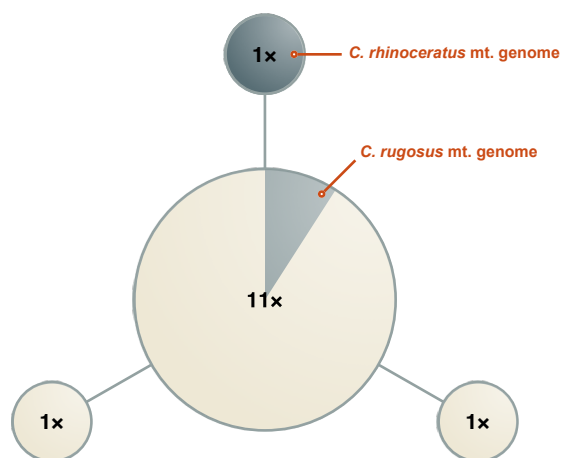


Figure 7 Haplotype genealogy graph for CO1. Circles represent four distinct *Channichthys* CO1 haplotypes, found in 13 *C. rhinoceras* and one *C. rugosus* individuals. Radii are drawn according to the number of individuals with that haplotype (indicated with labels on circles). Edges represent substitutions. Each of the three edges has a length of one substitution. mt., mitochondrial.

haplochromine cichlids (Meier et al., 2017). In that case low mitochondrial diversity and rampant haplotype sharing would conceal a large species diversity. It would need to be tested using genome-wide nuclear data if such a scenario applies to *Channichthys*, rather than a previous overestimation of species diversity in the genus.

Genetic data can be vital to corroborate or reject taxonomic assessments based on morphology and to more accurately estimate organismal diversity. The fixation of specimens with formalin, which severely hampers genetic analyses, has long been recognized, and indeed lamented, as a major obstacle for tapping the theoretically vast potential of museum collections for addressing

Table 3 Within-species mitochondrial sequence divergence in Notothenioidei and between-species divergence for closely-related Channichthyidae

Species	Accessions	# s.	# i.	# s. ¹	# i. ¹
<i>Trematomus borchgrevinki</i>	NC_030320, KX025131	92	22	69	8
<i>Notothenia coriiceps</i>	NC_015653, AP006021	16	3	12	2
<i>Notothenia rossii</i>	NC_050685, MT192936	22	15	11	4
<i>Chaenodraco wilsoni</i>	NC_039158, MT559885	48	11	33	10
<i>Chionodraco hamatus</i>	NC_029737, KU341409	55	13	42	5
<i>Chionodraco hamatus</i> , <i>Chionodraco rastrorpinosus</i>	NC_029737, NC_039543	421	25	253	6
<i>Chionobathyscus dewitti</i> , <i>Cryodraco antarcticus</i>	NC_046762, NC_045285	540	34	272	11
<i>Channichthys rhinoceratus</i> , <i>Channichthys rugosus</i>	NC_057120, new	26 ²	0 ²	17	0

s., substitutions; i., indels.

¹Excluding the *ND6* / D-loop region.

²Potentially incomplete due to two gaps in the *C. rugosus* sequence within the *ND6* / D-loop region.

long standing questions in systematics, taxonomy, evolutionary and conservation biology (Card, Shapiro, Giribet, Moritz, & Edwards, 2021; Raxworthy & Smith, 2021). Time-structured samples, including extinct species, can reveal details about the recent decline of biodiversity. Specimens from places that are difficult to access could fill gaps in studies otherwise relying on a smaller geographic sampling. Given this potential it is unsurprising that the research community continues to undertake great efforts in refining methodology to maximise the data yield from wet-collection specimens (Campos & Gilbert, 2012; Hahn et al., 2021; Hykin, Bi, & Mcguire, 2015; Schander & Kenneth, 2003; Straube et al., 2021). Here, we demonstrated that recently proposed methods that build on advances in the study of ancient DNA and high-throughput shotgun sequencing can recover usable genetic data from a formalin-fixed fish specimen. The short molecule lengths and very low DNA amounts recovered from such samples mandate the use of specialised, sensitive methods, such as lower centrifugation speeds and greater excess of binding buffer in DNA extraction (Dabney et al., 2013). The chemical cross-linking of DNA with DNA and proteins requires a harsher treatment of the tissue sample during lysis, for example by using high amounts of proteinase, as done here. Subsequently, the use of very efficient single-stranded DNA library preparation can convert appreciable numbers of molecules even if chemical damage and cross-linking are prevalent. Caution should be taken when analysing such low-yield samples, as levels of contamination regarded minor in other circumstances can obscure signal from the target or lead to incorrect interpretations. Working in a clean laboratory that is dedicated to the analysis of low-biomass,

degraded samples is therefore recommended, as well as including appropriate negative controls to monitor contamination. This extra effort, however, is greatly rewarded when open questions can be addressed with otherwise unobtainable data.

Code Availability. Analysis code is available from GitHub (<https://github.com/mmatschiner/unsequenced>).

Acknowledgments. We thank Arcady V. Balushkin for providing the *C. rugosus* specimen and Marcelo Sánchez-Villagra for financially supporting the sequencing of its mitochondrial genome. Supto Andriyono and Hyun-Woo Kim provided helpful information about the *C. rhinoceratus* mitochondrial genome. Mark Lever (ETH Zurich) kindly provided lab space. The Genetic Diversity Centre (ETH Zurich) provided access to laboratory and HPC facilities. The Functional Genomics Centre Zürich (ETH and University of Zurich) provided assistance with sequencing.

Author Contributions. M.Mu. performed molecular lab work, bioinformatic analyses, and contributed to the manuscript. E.N. initiated the study and contributed the tissue sample of *C. rugosus*. L.R. established the collaboration. M.Ma. performed bioinformatic analyses and wrote most of the manuscript. All authors read and approved the final version of the manuscript.

Funding. M. Muschick was supported by the SNSF Sinergia grant CR-SII5_183566. M. Matschiner was supported by the Norwegian Research Council with FRIPRO grant 275869. E. Nikolaeva was supported by a research programme of the Zoological Institute of the Russian Academy of Sciences (project number 122031100285-3).

Declarations

Conflict of interest. The authors declare that no competing interest exists, as well as that there is no financial support or relationships that may pose any kind of conflict. Likewise, the authors declare that contributed to the text, agreed with its content and approved it for submission.

References

- Allen, J.M., LaFrance, R., Folk, R.A., Johnson, K.P., Guralnick, R.P. (2018). aTRAM 2.0: An improved, flexible locus assembler for NGS data. *Evolutionary Bioinformatics*, 14, 1176934318774546.
10.1177/1176934318774546
- Altschul, S.F., Gish, W., Miller, W., Myers, E.W., Lipman, D.J. (1990). Basic local alignment search tool. *Journal of Molecular Biology*, 215(3), 403–410.

- 783
784 10.1016/s0022-2836(05)80360-2
785
- 786 Andriyono, S., Alam, M.J., Lee, S.R., Choi, S.-G., Chung, S., Kim, H.-W.
787 (2019, July). Characterization of the complete mitochondrial genome of
788 *Chionobathyscus dewitti* (Perciformes, Channichthyidae). *Mitochondrial*
789 *DNA Part B*, 4(2), 3914–3915.
- 790
791 10.1080/23802359.2019.1688112
- 792 Balushkin, A.V., & Nikolaeva, E.A. (2015). “Dolichobranchiata” muta-
793 tion in the Antarctic representatives from the families of plunderfishes
794 (Artedidraconidae) and white-blooded (Channichthyidae) fish (Notothe-
795 nioidei). *Journal of Ichthyology*, 55(1), 9–15.
- 796
797 10.1134/S0032945215010014
- 798
799 Buchfink, B., Xie, C., Huson, D.H. (2015). Fast and sensitive protein alignment
800 using DIAMOND. *Nature Methods*, 12(1), 59–60.
- 801
802 10.1038/nmeth.3176
- 803
804 Campos, P.F., & Gilbert, T.M.P. (2012). DNA extraction from formalin-fixed
805 material. *Methods in molecular biology (Clifton, N.J.)*, 840, 81–5.
- 806
807 10.1007/978-1-61779-516-9_11
- 808
809 Card, D.C., Shapiro, B., Giribet, G., Moritz, C., Edwards, S.V. (2021).
810 Museum Genomics. *Annual Review of Genetics*, 55(1), 1–27.
- 811
812 10.1146/annurev-genet-071719-020506
- 813
814 Chevreux, B., Wetter, T., Suhai, S. (1999). Genome sequence assembly using
815 trace signals and additional sequence information. *Computer Science*
816 *and Biology: Proceedings of the German Conference on Bioinformatics*
817 *(GCB)*, 1–12.
- 818
819
820 Clarke, A., & Johnston, I.A. (1996). Evolution and adaptive radiation of
821 antarctic fishes. *Trends in Ecology and Evolution*, 11(5), 212–218.
- 822
823 10.1016/0169-5347(96)10029-X
- 824
825 Colombo, M., Damerau, M., Hanel, R., Salzburger, W., Matschiner, M.
826 (2015). Diversity and disparity through time in the adaptive radiation
827 of Antarctic notothenioid fishes. *Journal of Evolutionary Biology*, 28(2),
828 376–394.

	829
10.1111/jeb.12570	830
	831
Dabney, J., Knapp, M., Glocke, I., Gansauge, M.-T., Weihmann, A., Nickel, B., ... Meyer, M. (2013, 09). Complete mitochondrial genome sequence of a Middle Pleistocene cave bear reconstructed from ultrashort DNA fragments. <i>Proceedings Of The National Academy Of Sciences Of The United States Of America</i> , 110(39), 15758 – 15763.	832
	833
	834
	835
	836
	837
10.1073/pnas.1314445110	838
	839
Duhamel, G., Gasco, N., & Davaine, P. (Eds.). (2005). <i>Poissons des Îles Kerguelen et Crozet. Guide Régional de l’Océan Austral. Patrimoines Naturels</i> (Vol. 63). Paris: Muséum National d’Histoire Naturelle.	840
	841
	842
Eastman, J.T. (2005). The nature of the diversity of Antarctic fishes. <i>Polar Biology</i> , 28(2), 93–107.	843
	844
	845
	846
10.1007/s00300-004-0667-4	847
	848
Eastman, J.T., & Eakin, R.R. (2021). Checklist of the species of notothenioid fishes. <i>Antarctic Science</i> , 33(3), 273–280.	849
	850
	851
10.1017/S0954102020000632	852
	853
Gansauge, M.-T., Aximu-Petri, A., Nagel, S., Meyer, M. (2020). Manual and automated preparation of single-stranded DNA libraries for the sequencing of DNA from ancient biological remains and other sources of highly degraded DNA. <i>Nature Protocols</i> , 15(8), 2279–2300.	854
	855
	856
	857
	858
10.1038/s41596-020-0338-0	859
	860
Gansauge, M.-T., Gerber, T., Glocke, I., Korlević, P., Lippik, L., Nagel, S., ... Meyer, M. (2017). Single-stranded DNA library preparation from highly degraded DNA using T4 DNA ligase. <i>Nucleic Acids Research</i> , gkx033.	861
	862
	863
	864
10.1093/nar/gkx033	865
	866
Gon, O., & Heemstra, P.C. (1990). <i>Fishes of the Southern Ocean</i> . Grahamstown, South Africa: J.L.B. Smith Institute of Ichthyology. (Pages: 196)	867
	868
	869
Gould, A.L., Fritts-Penniman, A., Gaisner, A. (2021). Museum genomics illuminate the high specificity of a bioluminescent symbiosis for a genus of reef fish. <i>Frontiers in Ecology and Evolution</i> , 9, 630207.	870
	871
	872
	873
10.3389/fevo.2021.630207	874

- 875 Grabherr, M.G., Haas, B.J., Yassour, M., Levin, J.Z., Thompson, D.A., Amit,
876 I., . . . Regev, A. (2011). Full-length transcriptome assembly from RNA-
877 Seq data without a reference genome. *Nature Biotechnology*, *29*(7), 644–
878 652.
879
880 10.1101/gr.229202
- 881
882 Hahn, E.E., Alexander, M.R., Grealy, A., Stiller, J., Gardiner, D.M., Holleley,
883 C.E. (2021). Unlocking inaccessible historical genomes preserved in
884 formalin. *Molecular Ecology Resources*.
885
886 10.1111/1755-0998.13505
- 887
888 Hureau, J.-C. (1964). Sur la probable identité des deux espèces du genre
889 *Chaenichthys*, de la famille des Channichthyidae (poissons à "sang
890 blanc"). *Bulletin du Muséum National d'Histoire Naturelle*, *36*(4),
891 450–456.
892
- 893
894 Huson, D.H., Beier, S., Flade, I., Górska, A., El-Hadidi, M., Mitra, S., . . .
895 Tappu, R. (2016). MEGAN Community Edition - interactive explo-
896 ration and analysis of large-scale microbiome sequencing data. *PLOS*
897 *Computational Biology*, *12*(6), e1004957.
898
899 10.1371/journal.pcbi.1004957
- 900
901 Hykin, S.M., Bi, K., Mcguire, J.A. (2015). Fixing Formalin:
902 A Method to Recover Genomic-Scale DNA Sequence Data from
903 Formalin-Fixed Museum Specimens Using High-Throughput Sequenc-
904 ing. *PLoS ONE*, *10*(10), e0141579 – 16. Retrieved from
905 <https://dx.plos.org/10.1371/journal.pone.0141579>
906
907 10.1371/journal.pone.0141579
- 908
909 Jónsson, H., Ginolhac, A., Schubert, M., Johnson, P.L.F., Orlando, L. (2013).
910 mapDamage2.0: fast approximate Bayesian estimates of ancient DNA
911 damage parameters. *Bioinformatics*, *29*(13), 1682 – 1684.
912
913 10.1093/bioinformatics/btt193
- 914
915 Kircher, M., Sawyer, S., Meyer, M. (2012). Double indexing overcomes inac-
916 curacies in multiplex sequencing on the Illumina platform. *Nucleic Acids*
917 *Research*, *40*(1), e3–e3.
918
919 10.1093/nar/gkr771
920

- Korneliussen, T.S., Albrechtsen, A., Nielsen, R. (2014). ANGSD: Analysis of next generation sequencing data. *BMC Bioinformatics*, 15(1), 356. 921
922
923
10.1186/s12859-014-0356-4 924
925
- Larsson, A. (2014). AliView: a fast and lightweight alignment viewer and editor for large datasets. *Bioinformatics*, 30(22), 3276–3278. (Publisher: Oxford University Press) 926
927
928
10.1093/bioinformatics/btu531 929
930
931
- Li, H., & Durbin, R. (2010). Fast and accurate long-read alignment with Burrows-Wheeler transform. *Bioinformatics*, 26(5), 589 – 595. 932
933
934
10.1093/bioinformatics/btp698 935
936
- Li, H., Handsaker, B., Wysoker, A., Fennell, T., Ruan, J., Homer, N., ... Subgroup, .G.P.D.P. (2009). The Sequence Alignment/Map format and SAMtools. *Bioinformatics*, 25(16), 2078–2079. 937
938
939
10.1093/bioinformatics/btp352 940
941
942
- Matschiner, M. (2016). Fitchi: haplotype genealogy graphs based on the Fitch algorithm. *Bioinformatics*, 32(8), 1250–1252. 943
944
945
10.1093/bioinformatics/btv717 946
947
- Matschiner, M., Colombo, M., Damerau, M., Ceballos, S., Hanel, R., Salzburger, W. (2015). The adaptive radiation of notothenioid fishes in the waters of Antarctica. *Extremophile Fishes: Ecology, Evolution, and Physiology of Teleosts in Extreme Environments* (Vol. 36). Cham: Springer International Publishing. 10.1111/j.1365-294X.2006.03105.x 948
949
950
951
952
- Meier, J.I., Marques, D.A., Mwaiko, S., Wagner, C.E., Excoffier, L., Seehausen, O. (2017). Ancient hybridization fuels rapid cichlid fish adaptive radiations. *Nature Communications*, 8, 14363. 953
954
955
10.1038/ncomms14363 956
957
958
- Meisner, E.E. (1974). New species of the icefishes from the Southern Ocean. *Vestnik Zoologii*, 6, 50–55. 959
960
961
962
- Minh, B.Q., Nguyen, M.A.T., von Haeseler, A. (2013). Ultrafast approximation for phylogenetic bootstrap. *Molecular Biology and Evolution*, 30(5), 1188–1195. 963
964
965
966

- 967 10.1093/oxfordjournals.molbev.a025811
968
969 Minh, B.Q., Schmidt, H.A., Chernomor, O., Schrempf, D., Woodhams, M.D.,
970 Von Haeseler, A., Lanfear, R. (2020). IQ-TREE 2: New models and
971 efficient methods for phylogenetic inference in the genomic era. *Molecular*
972 *Biology and Evolution*, 37(5), 1530–1534.
- 973 10.1093/molbev/msaa015
974
975 Near, T.J., Dornburg, A., Harrington, R.C., Oliveira, C., Pietsch, T.W.,
976 Thacker, C.E., ... Beaulieu, J.M. (2015). Identification of the notothe-
977 nioid sister lineage illuminates the biogeographic history of an Antarctic
978 adaptive radiation. *BMC Evolutionary Biology*, 15, 109.
- 980 10.1186/s12862-015-0362-9
981
982 Near, T.J., Dornburg, A., Kuhn, K.L., Eastman, J.T., Pennington, J.N., Patar-
983 nello, T., ... Jones, C.D. (2012). Ancient climate change, antifreeze,
984 and the evolutionary diversification of Antarctic fishes. *Proceedings of*
985 *the National Academy of Sciences USA*, 109(9), 3434–3439.
- 987 10.1073/pnas.1115169109
988
989 Near, T.J., MacGuigan, D.J., Parker, E., Struthers, C.D., Jones, C.D.,
990 Dornburg, A. (2018). Phylogenetic analysis of Antarctic notothe-
991 nioids illuminates the utility of RADseq for resolving Cenozoic adaptive
992 radiations. *Molecular Phylogenetics and Evolution*, 129, 268–279.
- 994 10.1016/j.ympev.2018.09.001
995
996 Nikolaeva, E.A. (2019). A review of the icefish species from the genus
997 *Channichthys* Richardson, 1844 (Channichthyidae) with double-rowed
998 gill rakers. *Proceedings of the Zoological Institute RAS*, 323(4), 558–567.
- 1000 10.31610/trudyzin/2019.323.4.558
1001
1002 Nikolaeva, E.A. (2020). Redescription of the unicorn icefish *Channichthys*
1003 *rhinocerotus* Richardson (Notothenioidei: Channichthyidae) with syn-
1004 onymization of three similar species. *Proceedings of the Zoological*
1005 *Institute RAS*, 324(4), 485–496.
- 1006 10.31610/trudyzin/2020.324.4.485
1007
1008
1009 Nikolaeva, E.A. (2021). On the taxonomic status of the red icefish *Chan-*
1010 *nichthys rugosus* (Notothenioidei: Channichthyidae) from the Kerguelen
1011 Islands (South Ocean). *Proceedings of the Zoological Institute RAS*, 325,
1012 485–494.

	1013
10.31610/trudyzin/2021.325.4.485	1014
	1015
Nikolaeva, E.A., & Balushkin, A.V. (2019). Morphological characteristics of sailfish pike <i>Channichthys velifer</i> (Channichthyidae) from the Kerguelen Islands (Southern Ocean). <i>Journal of Ichthyology</i> , 59(6), 834–842.	1016
	1017
	1018
	1019
10.1134/S0032945219060079	1020
	1021
Norman, J.R. (1937). Fishes. B.A.N.Z. Antarctic Research Expedition 1929–31. <i>Repts Ser B Zool Bot</i> , 1(2), 50–88.	1022
	1023
	1024
	1025
Paijmans, J.L.A., Baleka, S., Henneberger, K., Taron, U.H., Trinks, A., Westbury, M.V., Barlow, A. (2017). Sequencing single-stranded libraries on the Illumina NextSeq 500 platform. <i>arXiv:1711.11004 [q-bio]</i> . Retrieved from http://arxiv.org/abs/1711.11004 (arXiv: 1711.11004)	1026
	1027
	1028
	1029
	1030
Papetti, C., Babbucci, M., Dettai, A., Basso, A., Lucassen, M., Harms, L., ... Negrisolo, E. (2021). Not Frozen in the Ice: Large and Dynamic Rearrangements in the Mitochondrial Genomes of the Antarctic Fish. <i>Genome Biology and Evolution</i> , 13(3), evab017.	1031
	1032
	1033
	1034
	1035
10.1093/gbe/evab017	1036
	1037
Parker, E., Dornburg, A., Struthers, C.D., Jones, C.D., Near, T.J. (2022). Phylogenomic species delimitation dramatically reduces species diversity in an Antarctic adaptive radiation. <i>Systematic Biology</i> , 71(1), 58–77.	1038
	1039
	1040
	1041
10.1093/sysbio/syab057	1042
	1043
Raxworthy, C.J., & Smith, B.T. (2021). Mining museums for historical DNA: advances and challenges in museomics. <i>Trends in Ecology & Evolution</i> , 36(11), 1049–1060.	1044
	1045
	1046
	1047
10.1016/j.tree.2021.07.009	1048
	1049
Regan, C.T. (1913). II. – The Antarctic fishes of the Scottish National Antarctic expedition. <i>Transactions of the Royal Society of Edinburgh: Earth Sciences</i> , 49(2), 229–292.	1050
	1051
	1052
	1053
	1054
Richardson, J. (1844, June). LII.— <i>Descriptions of a new Genus of Gobioid Fish</i> . <i>Annals and Magazine of Natural History</i> , 13(86), 461–462.	1055
	1056
	1057
10.1080/03745484409442631	1058

- 1059 Rüber, L., & Zardoya, R. (2005). Rapid cladogenesis in marine fishes revisited.
1060 *Evolution*, 59(5), 1119–1127.
1061
1062 10.1111/j.0014-3820.2005.tb01048.x
1063
- 1064 Schander, C., & Kennen, H.M. (2003, 01). DNA, PCR and formalized
1065 animal tissue – a short review and protocols. *Organisms Diversity &*
1066 *Evolution*, 3(3), 195–205.
1067
1068 10.1078/1439-6092-00071
1069
- 1070 Schiavon, L., Dulière, V., La Mesa, M., Marino, I.A.M., Codogno, G., Boscari,
1071 E., ... Papetti, C. (2021). Species distribution, hybridization and con-
1072 nectivity in the genus *Chionodraco* : Unveiling unknown icefish diversity
1073 in antarctica. *Diversity and Distributions*, 27(5), 766–783.
1074
1075 10.1111/ddi.13249
1076
- 1077 Shandikov, G.A. (1995a). A new species of icefish, *Channichthys panti-*
1078 *capei* sp. n. (Channichthyidae, Notothenioidei) from the Kerguelen Island
1079 (Antarctica). *Proceedings of South Research Institute of Marine Fishery*
1080 *and Oceanography (YugNIRO), Special Issue, 1*, 1–10.
1081
- 1082 Shandikov, G.A. (1995b). To the question about the composition of icefish
1083 species of the genus *Channichthys* in the Kerguelen Islands area with
1084 description of three new species. *Proceedings of South Research Institute*
1085 *of Marine Fishery and Oceanography (YugNIRO), Special Issue, 2*, 1–18.
1086
1087
- 1088 Shandikov, G.A. (2008). *Channichthys mithridatis*, a new species of icefishes
1089 (Perciformes: Notothenioidei: Channichthyidae) from the Kerguelen Is-
1090 lands (East Antarctica), with comments on the taxonomic status of
1091 *Channichthys normani*. *Visnyk Charkivs'koho Universytetu Imeni V. N.*
1092 *Karazina, Ser. Biologija, Charkiv*, 14(917), 123–131.
1093
1094
- 1095 Shandikov, G.A. (2011). *Channichthys richardsoni* sp. n., a new Antarctic
1096 icefish (Perciformes: Notothenioidei: Channichthyidae) from the Kergue-
1097 len Islands area, Indian sector of the Southern Ocean. *Journal of V. N.*
1098 *Karazin Kharkiv National University, Series: Biology*(14), 125–134.
1099
1100
- 1101 Smith, P.J., Steinke, D., Dettai, A., McMillan, P., Welsford, D., Stewart, A.,
1102 Ward, R.D. (2012, September). DNA barcodes and species identifications
1103 in Ross Sea and Southern Ocean fishes. *Polar Biology*, 35(9), 1297–1310.
1104

10.1007/s00300-012-1173-8	1105
	1106
Spodareva, V.V., & Balushkin, A.V. (2014, January). Description of a new species of plunderfish of genus <i>Pogonophryne</i> (Perciformes: Artedidraconidae) from the Bransfield Strait (Antarctica) with a key for the identification of species of the group “marmorata”. <i>Journal of Ichthyology</i> , 54(1), 1–6.	1107
	1108
	1109
	1110
	1111
	1112
10.1134/S0032945214010135	1113
	1114
Straube, N., Lyra, M.L., Paijmans, J.L.A., Preick, M., Basler, N., Penner, J., ... Hofreiter, M. (2021). Successful application of ancient DNA extraction and library construction protocols to museum wet collection specimens. <i>Molecular Ecology Resources</i> , 21(7), 2299–2315.	1115
	1116
	1117
	1118
	1119
10.1111/1755-0998.13433	1120
	1121
	1122
	1123
	1124
	1125
	1126
	1127
	1128
	1129
	1130
	1131
	1132
	1133
	1134
	1135
	1136
	1137
	1138
	1139
	1140
	1141
	1142
	1143
	1144
	1145
	1146
	1147
	1148
	1149
	1150